Quantum-mechanical noise in an interferometer

Carlton M. Caves

W. K. Kellogg Radiation Laboratory, California Institute of Technology, Pasadena, California 91125

(Received 15 August 1980)

The interferometers now being developed to detect gravitational waves work by measuring the relative positions of widely separated masses. Two fundamental sources of quantum-mechanical noise determine the sensitivity of such an interferometer: (i) fluctuations in number of output photons (photon-counting error) and (ii) fluctuations in radiation pressure on the masses (radiation-pressure error). Because of the low power of available continuous-wave lasers, the sensitivity of currently planned interferometers will be limited by photon-counting error. This paper presents an analysis of the two types of quantum-mechanical noise, and it proposes a new technique—the "squeezed-state" technique—that allows one to decrease the photon-counting error while increasing the radiation-pressure error, or vice versa. The key requirement of the squeezed-state technique is that the state of the light entering the interferometer's normally unused input port must be not the vacuum, as in a standard interferometer, but rather a "squeezed state"—a state whose uncertainties in the two quadrature phases are unequal. Squeezed states can be generated by a variety of nonlinear optical processes, including degenerate parametric amplification.

I. INTRODUCTION

The task of detecting gravitational radiation is driving dramatic improvements in a variety of technologies for detecting very weak forces.[1] These improvements are forcing a careful examination of quantum-mechanical limits on the accuracy with which one can monitor the state of a macroscopic body on which a weak force acts.[2] One promising technology uses an interferometer to monitor the relative positions of widely separated masses. This paper analyzes the quantum-mechanical limits on the performance of interferometers, and it introduces a new technique that might lead to improvements in their sensitivity.

The prototypal interferometer for gravitational-wave detection is a two-arm, multireflection Michelson system, powered by a laser (see Fig. 3 below). The intensity in either of the interferometer's output ports provides information about the difference $z \equiv z_2 - z_1$ between the end mirrors' positions relative to the beam splitter, and changes in z reveal the passing of a gravitational wave. The first interferometer for gravitational-wave detection was built and operated at the Hughes Research Laboratories in Malibu, California, in the early 1970's (Ref. 3); this first effort was small-scale and had modest sensitivity. Now several groups around the world are developing interferometers of greatly improved sensitivity.[4-6] A long-range goal is to construct large-scale interferometers, with baselines $l \sim 1$ km, in order to achieve a strain sensitivity $\Delta z/l \sim 10^{-21}$ for frequencies from about 30 Hz to 10 kHz. This sensitivity goal is based on estimates for the strength of gravitational waves that pass the Earth reasonably often.[1]

It has been known for some time that quantum mechanics limits the accuracy with which an interferometer can measure z—or, indeed, the accuracy with which any position-sensing device can determine the position of a free mass.[2,5,7] In a measurement of duration τ, the probable error in the interferometer's determination of z can be no smaller than the "standard quantum limit":

$$(\Delta z)_{\text{SQL}} = (2\hbar\tau/m)^{1/2}, \qquad (1.1)$$

where m is the mass of each end mirror [$(\Delta z)_{\text{SQL}} \sim 6 \times 10^{-18}$ cm for $m \sim 10^5$ g, $\tau \sim 2 \times 10^{-3}$ sec]. The validity of the standard quantum limit is unquestionable, resting as it does solely on the Heisenberg uncertainty principle applied to the quantum-mechanical evolution of a free mass.

The standard quantum limit for an interferometer can also be obtained from a more detailed argument[5,8-10] that balances two sources of error: (i) the error in determining z due to fluctuations in the number of output photons (photon-counting error) and (ii) the perturbation of z during a measurement produced by fluctuating radiation-pressure forces on the end mirrors (radiation-pressure error). As the input laser power P increases, the photon-counting error decreases, while the radiation-pressure error increases. Minimizing the total error with respect to P yields a minimum error of order the standard quantum limit and an optimum input power[9,11]

$$P_0 \simeq \tfrac{1}{2}(mc^2/\tau)(1/\omega\tau)(1/b^2) \qquad (1.2)$$

at which the minimum error can be achieved. Here ω is the angular frequency of the light, and b is the number of bounces at each end mirror.

At the optimum power the photon-counting and radiation-pressure errors are equal.

The original argument[8] leading to the optimum power (1.2) attributed the radiation-pressure fluctuations that perturb z to fluctuations in input power. Some later versions of the argument were unclear about the source of the relevant radiation-pressure fluctuations.[5,9] As a result, the argument had always been under suspicion,[8] because fluctuations in input power should divide equally at the beam splitter and, therefore, should have no effect on z. This suspicion led to a "lively but unpublished controversy"[6] over the existence of a radiation-pressure force that affects z and, consequently, over the existence of an optimum laser power.

In a recent paper I resolved this controversy.[11] There I pointed out that the relevant radiation-pressure force has nothing to do with input power fluctuations; instead, it can be attributed to vacuum (zero-point) fluctuations in the electromagnetic field, which enter the interferometer from the unused input port (direction of dashed arrow in Fig. 3 below). When superposed on the input laser light, these fluctuations produce a fluctuating force that perturbs z. (An alternative and equivalent point of view attributes the relevant radiation-pressure fluctuations to random scattering of the input photons at the beam splitter.[10,11]) In the same paper I claimed that these vacuum fluctuations (not input power fluctuations) are also responsible for the unavoidable fluctuations in number of output photons.

A reasonable set of values for the interferometer's parameters, which I shall use as a fiducial set throughout this paper, is $m \sim 10^5$ g, $\tau \sim 2 \times 10^{-3}$ sec, $\omega \sim 4 \times 10^{15}$ rad sec^{-1} (wavelength $\lambda \sim 5000$ Å), and $b \sim 200$. For these values P_0 is approximately 8×10^3 W — a power far higher than powers of present continuous-wave lasers. The low available input power means that the interferometers now planned for use as gravitational-wave detectors will be limited not by the standard quantum limit, but rather by $1/\sqrt{N}$ photon-counting statistics. In this paper I address this problem by introducing a new technique, which in principle allows an interferometer to achieve the quantum-limited position sensitivity (1.1) for input powers far less than P_0.

Perhaps suprisingly, this new technique does not require modifying the input laser light; instead, it requires modifying the light entering the normally unused input port. Specifically, the unused port must see not the vacuum (ground) state of the electromagnetic field, but rather a "squeezed state"—a state whose fluctuations in one quadrature phase are less than zero-point fluctuations (or the fluctuations in any coherent state), and whose fluctuations in the other phase are greater than zero-point fluctuations. This technique works because one of the two phases is responsible for the fluctuations in number of output photons, while the other is responsible for the radiation-pressure fluctuations that perturb z. Thus, by "squeezing the vacuum" before it can enter the normally unused input port, one can reduce the photon-counting error (i.e., beat $1/\sqrt{N}$ photon-counting statistics) at the expense of increasing the radiation-pressure error, or vice versa.

In practice, this squeezed-state technique is not likely to allow gravitational-wave interferometers to operate at the standard quantum limit. However, it might allow a given underpowered interferometer to achieve a somewhat better sensitivity, without changes in its input power or any of its other parameters. Unfortunately, the usefulness of the squeezed-state technique is likely to be severely limited by the losses in real mirrors, which destroy the crucial feature of the technique—the reduced noise in one of the two quadrature phases. The technique can be useful only in interferometers whose performance is not limited by losses in the mirrors.

This paper extends and refines the analysis given in Ref. 11, and it introduces the new squeezed-state technique. Section II gives a detailed analysis of the quantum-mechanical noise in an interferometer, with emphasis on the theoretical capabilities of the squeezed-state technique. Section II A presents some formal considerations that facilitate handling various states of the electromagnetic field, including squeezed states. Section II B begins by presenting an idealized model of an interferometer and an outline of the procedures used in the subsequent analysis, and it then proceeds to that analysis. Specifically, the radiation-pressure fluctuations, the output fluctuations in number of photons, the optimum sensitivity, and the optimum power are analyzed for an interferometer that has either vacuum or a squeezed state incident on the normally unused input port. Along the way the intensity-correlation properties of the light in the two arms of the interferometer are investigated. Section III focuses on more practical matters, with emphasis on application of the squeezed-state technique to real interferometers, which are limited by photon-counting statistics. Section III reviews a method for generating squeezed states using an optical degenerate parametric amplifier, it investigates the limitations imposed by mirror losses, and it proposes a method for

doing the photon counting that can realize the potential reduction in photon-counting error even with inefficient photodetectors. Section IV comments briefly on the results and their relevance to gravitational-wave detection.

II. ANALYSIS OF QUANTUM-MECHANICAL NOISE IN AN INTERFEROMETER

A. Formal considerations

Before turning to a detailed analysis of an interferometer, it is useful to review some properties of various special states of a harmonic oscillator. These states play a crucial role in the subsequent analysis.

Consider a single mode of the electromagnetic field with angular frequency ω, and let a and $a^\dagger$ be its annihilation and creation operators ($[a, a^\dagger] = 1$). Then the operator for the number of photons in the mode is

$$N = a^\dagger a, \tag{2.1}$$

and a dimensionless complex-amplitude operator for the mode is

$$X_1 + iX_2 = a. \tag{2.2}$$

The Hermitian operators X_1 and X_2 (real and imaginary parts of the complex amplitude) give dimensionless amplitudes for the mode's two quadrature phases. The commutation relation for a and $a^\dagger$ implies a corresponding commutation relation for X_1 and X_2: $[X_1, X_2] = i/2$. The resulting uncertainty principle is $\Delta X_1 \Delta X_2 \geq \frac{1}{4}$.

The complex amplitude of a single mode is a constant of the motion—i.e., it is constant in the Heisenberg picture. Thus, in Eq. (2.2), X_1 and X_2 are Heisenberg-picture operators, whereas a is a Heisenberg-picture operator evaluated at a particular time (or, equivalently, a Schrödinger-picture operator). There is a phase ambiguity in the relation between the complex amplitude and the annihilation operator; this phase ambiguity corresponds to the freedom to make rotations in the complex-amplitude plane (or to freedom in the choice of fiducial time in the relation between $X_1 + iX_2$ and a).

A particularly useful set of states for the electromagnetic field is the set of coherent states introduced by Glauber.[12] These states are most easily generated using the unitary displacement operator[12]:

$$D(\alpha) \equiv \exp(\alpha a^\dagger - \alpha^* a) = e^{-|\alpha|^2/2} e^{\alpha a^\dagger} e^{-\alpha^* a}, \tag{2.3}$$

where α is an arbitrary complex number. Note that $D^\dagger(\alpha) = D^{-1}(\alpha) = D(-\alpha)$. The most useful property of the displacement operator is the way it transforms a and $a^\dagger$:

$$D^\dagger(\alpha) a D(\alpha) = a + \alpha,$$

$$D^\dagger(\alpha) a^\dagger D(\alpha) = a^\dagger + \alpha^*. \tag{2.4}$$

By displacing the vacuum (ground) state $|0\rangle$, one obtains the *coherent state* $|\alpha\rangle$:

$$|\alpha\rangle \equiv D(\alpha)|0\rangle = e^{-|\alpha|^2/2} e^{\alpha a^\dagger}|0\rangle. \tag{2.5}$$

The expectation values and variances of X_1, X_2, and N in a coherent state are given by

$$\langle X_1 + iX_2 \rangle = \alpha, \quad \Delta X_1 = \Delta X_2 = \tfrac{1}{2},$$

$$\langle N \rangle = |\alpha|^2, \quad \Delta N = |\alpha|. \tag{2.6}$$

The coherent state $|\alpha\rangle$ has mean complex amplitude α, and it is a minimum-uncertainty (Gaussian) state for X_1 and X_2, with equal uncertainties in the two quadrature phases. A coherent state is conveniently represented by an "error circle" in a complex-amplitude plane whose axes are X_1 and X_2 [see Fig. 1(a)]. The center of the error circle lies at $\langle X_1 + iX_2 \rangle = \alpha$, and the radius $\Delta X_1 = \Delta X_2 = \tfrac{1}{2}$ accounts for the uncertainties in X_1 and X_2.

Squeezed states constitute another useful set of states. They are conveniently generated by using the unitary *squeeze operator*[13-15]:

$$S(\zeta) \equiv \exp[\tfrac{1}{2}\zeta^* a^2 - \tfrac{1}{2}\zeta(a^\dagger)^2], \quad \zeta = re^{i\theta}, \tag{2.7}$$

where ζ is an arbitrary complex number. The squeeze operator was introduced by Stoler,[13] and the name was coined by Hollenhorst.[15] Note that $S^\dagger(\zeta) = S^{-1}(\zeta) = S(-\zeta)$. The most useful unitary transformation properties of the squeeze operator are

$$S^\dagger(\zeta) a S(\zeta) = a \cosh r - a^\dagger e^{i\theta} \sinh r,$$

$$S^\dagger(\zeta) a^\dagger S(\zeta) = a^\dagger \cosh r - a e^{-i\theta} \sinh r,$$

$$S^\dagger(\zeta)(Y_1 + iY_2)S(\zeta) = Y_1 e^{-r} + iY_2 e^r, \tag{2.8}$$

where

$$Y_1 + iY_2 = (X_1 + iX_2)e^{-i\theta/2} \tag{2.9}$$
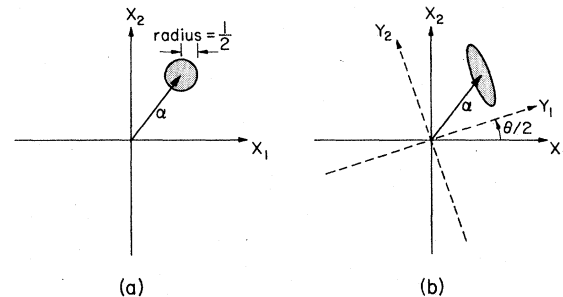

(a)   (b)

FIG. 1. (a) Error circle in complex-amplitude plane for coherent state $|\alpha\rangle$. (b) Error ellipse in complex-amplitude plane for squeezed state $|\alpha, re^{i\theta}\rangle$ ($r > 0$).

is a rotated complex amplitude. The squeeze operator attenuates one component of the (rotated) complex amplitude, and it amplifies the other component. The degree of attenuation and amplification is determined by $r = |\zeta|$, which therefore will be called the *squeeze factor*.

The *squeezed state* $|\alpha, \zeta\rangle$ is obtained by first squeezing the vacuum and then displacing it:

$$|\alpha, \zeta\rangle \equiv D(\alpha)S(\zeta)|0\rangle . \tag{2.10}$$

Note that $|\alpha, 0\rangle = |\alpha\rangle$. The most important expectation values and variances for a squeezed state are

$$\langle X_1 + iX_2\rangle = \langle Y_1 + iY_2\rangle e^{i\theta/2} = \alpha ,$$

$$\Delta Y_1 = \tfrac{1}{2}e^{-r}, \quad \Delta Y_2 = \tfrac{1}{2}e^r ,$$

$$\langle N\rangle = |\alpha|^2 + \sinh^2 r , \tag{2.11}$$

$$(\Delta N)^2 = |\alpha \cosh r - \alpha^* e^{i\theta} \sinh r|^2$$

$$+ 2\cosh^2 r \sinh^2 r .$$

The squeezed state $|\alpha, \zeta\rangle$ has the same expected complex amplitude as the corresponding coherent state $|\alpha\rangle$, and it is a minimum-uncertainty (Gaussian) state for Y_1 and Y_2. The difference lies in its unequal uncertainties for Y_1 and Y_2. In the complex-amplitude plane, the coherent-state error circle has been "squeezed" into an "error ellipse" of the same area [see Fig. 1(b)]. The principal axes of the ellipse lie along the Y_1 and Y_2 axes, and the principal radii are ΔY_1 and ΔY_2.

Squeezed states were introduced by Stoler,[13,16] who called them "minimum-uncertainty packets." They have since been considered by Lu[14,17] ("new coherent states"), by Yuen[18,19] ("two-photon coherent states"), and by Hollenhorst[15] ("wave-packet states"). Yuen, in particular, has examined in detail the properties of squeezed states.[19] The reduced uncertainty in one quadrature phase of a squeezed state is obviously attractive for optical communications purposes; in a recent series of papers,[20-22] Yuen and his collaborators have considered this application of squeezed states and have given detailed analyses of several photo-detection techniques applied to squeezed states.

Squeezed states have also found application in the theory of mechanically resonant gravitational-wave detectors. A detector of this type[1] is a macroscopic mechanical system (usually a massive cylinder of aluminum); a gravitational wave betrays its presence by changing the complex amplitude of oscillation of some mode of the mechanical system (usually the fundamental mode). A fundamental theoretical problem has been how to monitor the mode of interest in a way that allows detection of gravitational waves so weak that they change the complex amplitude

of that mode by less than the width of a coherent state. This problem has become known as the "quantum nondemolition" problem, and solutions to it are known as quantum nondemolition measurement techniques. The quantum nondemolition problem and its solutions have been analyzed extensively (see Ref. 2 and references cited therein). It should not be surprising that squeezed states, with their reduced uncertainty in one component of the complex amplitude, play a key role in one quantum nondemolition technique, the "back-action-evading" method of making quantum nondemolition measurements.[2] In the back-action-evading method one designs a measuring device that monitors only one component of the relevant mode's complex amplitude; this device automatically forces that mode into a state similar to a squeezed state.

To better visualize the properties of coherent and squeezed states, it is perhaps useful to consider the time dependences of the expectation value and variance of a field quantity, such as the electric field $E(t)$. These time dependences are easily read off the complex-amplitude plots in Fig. 1; a complex-amplitude plane whose axes are E and $\dot{E}$ must rotate with angular velocity ω relative to the (X_1, X_2) phase plane, in order to produce a sinusoidal oscillation of the expectation value of E. For a coherent state the rotation of the error circle leads to a constant value for the variance of the electric field [see Fig. 2 (a)]. For a squeezed state, however, the rotation of the error ellipse leads to a variance that oscillates with frequency 2ω. This situation is depicted in Fig. 2 for two cases: the case where the coherent excitation of the mode appears in the quadrature phase that has reduced noise [Fig. 2(b)] and the case where the coherent excitation appears in the quadrature phase that has increased noise [Fig. 2(c)].

B. Detailed analysis of an interferometer

1. Model interferometer and outline of analysis

A typical interferometer for gravitational-wave detection is a multireflection Michelson system of the sort sketched in Fig. 3 (Refs. 4-6,8). An idealized version of such an interferometer works as follows. Light enters the interferometer from a laser, is split at a lossless, 50-50 beam splitter, bounces back and forth many times between perfectly reflecting mirrors in the nearly equal-length arms, and finally is recombined at the beam splitter. The number of bounces at each end mirror is denoted by b. The end mirrors are attached to large masses, each of mass m. The beam splitter and the inner mirrors are
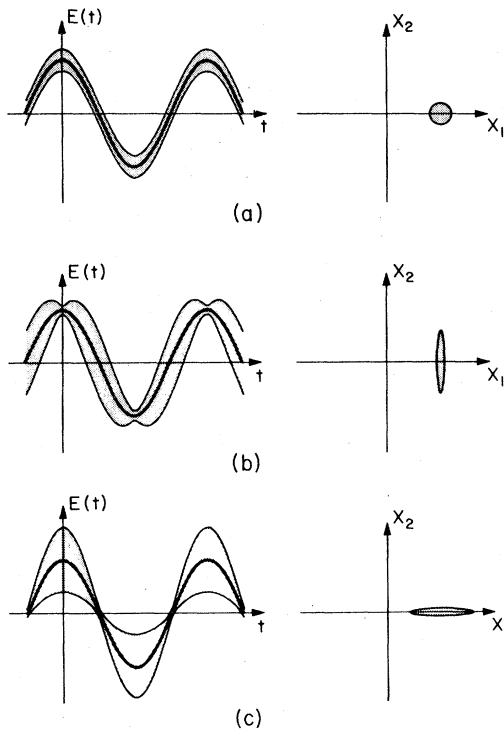
FIG. 2. Graphs of electric field versus time for three states of the electromagnetic field. In each graph the dark line is the expectation value of the electric field, and the shaded region represents the uncertainty in the electric field. To the right of each graph is the corresponding "error box" in the complex-amplitude plane. (a) Coherent state $|\alpha\rangle$ (α real). This state exhibits neither bunching nor antibunching ($g_{12}^{(2)}=1$). (b) Squeezed state $|\alpha,r\rangle$ (α real) with $r>0$. This state exhibits antibunching ($g_{12}^{(2)}<1$) as long as $0<r\lesssim\frac{1}{4}\ln(8\alpha^2)$. (c) Squeezed state $|\alpha,r\rangle$ (α real) with $r<0$. This state exhibits bunching.

rigidly attached to one another and to a mass M. For simplicity I assume $M\gg m$, so that the radiation-pressure-induced motion of the beam splitter can be ignored and the beam splitter can be regarded as at rest. Each arm of the interferometer has a fiducial length l, and the displacements of the end mirrors from their fiducial positions are denoted z_1 and z_2.

The intensity in one—or perhaps both—of the output ports is measured by an ideal photodetector (quantum efficiency one), and this measurement provides information about the difference $z\equiv z_2-z_1$ between the positions of the end mirrors. The information about z is not the instantaneous value; rather, it is some sort of average of z over the storage time—the time $\tau_s=2bl/c$ the light spends in each arm. Thus the storage time defines the interferometer's time resolution; the best sensitivity is achieved when the measurement time τ— the time over which one averages the output
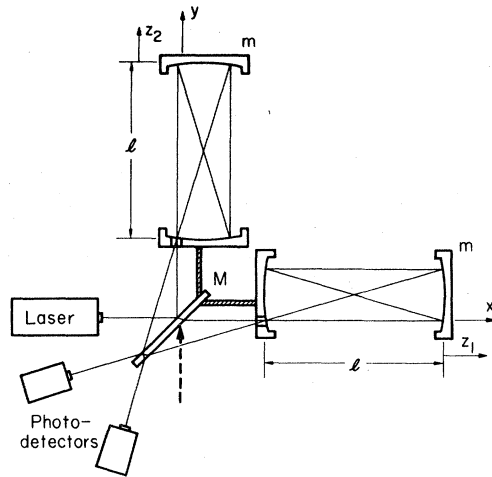

FIG. 3. Schematic diagram of Michelson interferometer ($b=2$) described in text.

to get a value for z—is approximately equal to τ_s. For a baseline $l\sim1$ km and $b\sim200$, $\tau_s\sim10^{-3}$ sec. Throughout the following analysis I assume $\tau_s\lesssim\tau$.

The most important idealizations in this model are the assumptions of lossless mirrors and ideal photodetectors. The consequences of relaxing these two assumptions are considered in Sec. III.

The goal of this section is to analyze the quantum-mechanical limits on the performance of an interferometer. The philosophy is ruthless simplification: throw away all details not necessary for understanding the fundamental limits. The quantum-mechanical uncertainty in the interferometer's determination of z can be thought of as coming from three sources: (i) the intrinsic quantum-mechanical uncertainties in the end mirrors' positions and momenta; (ii) the perturbations of the end mirrors' positions by radiation-pressure fluctuations (radiation-pressure error); and (iii) the fluctuations in number of photons at the output ports (photon-counting error). In reality, all three sources of error manifest themselves in the same way—by feeding into the interferometer's output and producing fluctuations in that output. A complete analysis must consider all three simultaneously.[23] Nonetheless, the division of the total uncertainty is a useful conceptual device, and it serves as the basis of the simplified approach adopted here: calculate the error produced by each type of uncertainty separately, and then assume that the total error is the quadrature sum of the separate errors.

The intrinsic quantum-mechanical uncertainties in the end mirrors' positions and momenta can be dealt with most easily. They feed into the

interferometer's output and degrade its deter-
mination of z. In the best case these uncertainties
enforce a minimum error in z given by the stan-
dard quantum limit (1.1).[2, 5, 7] These uncertainties
and the limits they impose on measurements of
z are well understood; consequently, they need
not be considered here—i.e., the end mirrors
are treated as classical, rather than quantum-
mechanical, objects.

The radiation-pressure error is obtained using
the following simple procedure. The momentum
transferred to the end masses is calculated as-
suming the end masses remain at rest throughout
the measurement—i.e., assuming $m \to \infty$. Since
the end masses really do move, the actual momen-
tum transferred will be slightly different because
of the Doppler shift of the reflected radiation;
this difference is negligible for the cases of in-
terest. The perturbation of z produced by the
momentum transferred is estimated by reverting
to finite masses m and allowing the end mirrors
to move. This perturbation of z feeds into the
interferometer's output and produces a compar-
able error in determining z.

In much the same way the fluctuations in num-
ber of output photons are determined assuming
the end mirrors are at rest. These fluctuations
are then converted into the photon-counting error
by considering differences between neighboring
$z = $const configurations. This procedure ignores
the complicated averaging produced by the storage
time, but it retains the essential features of the
output fluctuations in number of photons.

The above-outlined assumptions allow a further
drastic simplification. Instead of dealing with
beams of finite size and finite duration, I can
restrict attention to only a small number of
plane-wave modes of the electromagnetic field.
In addition, I ignore the small angular deviations
in the directions of the beams—i.e., I assume
that the plane-wave modes propagate precisely
along the directions of the x and y axes of Fig. 3.

2. Radiation-pressure error and second-order coherence

With the above assumptions one can calculate
the momentum transferred to each end mirror
quite simply. One finds the momentum carried
by the light in each arm of the interferometer;
the momentum transferred at each bounce is
twice this amount.

Carrying out this procedure requires only four
modes of the electromagnetic field in the presence
of the beam splitter ("beam-splitter modes").
The first two modes of interest are "in" modes—
modes appropriate for constructing precollision
wave packets that scatter off the beam splitter.
Thus they are in states in the sense of scattering

theory. The first mode of interest (mode 1^+)
describes light incident from the input (laser)
port. It consists of an incident plane wave with
angular frequency ω, propagating inward along
the x axis, and scattered waves propagating along
the two arms of the interferometer. The second
mode (mode 2^+) is the corresponding in mode
that describes light incident from the normally
unused input port (light incident along the y axis;
direction of dashed arrow in Fig. 3). Outside
the beam splitter the electric fields of these two
modes have the forms

$$E_1^+ = \begin{cases} \mathcal{Q}e^{i(kx-\omega t)} - 2^{-1/2}\mathcal{Q}e^{i(\Delta-\mu)}e^{i(ky-\omega t)}, & y > x \\ 2^{-1/2}\mathcal{Q}e^{i\Delta}e^{i(kx-\omega t)}, & y < x \end{cases}$$

$$\tag{2.12}$$

$$E_2^+ = \begin{cases} 2^{-1/2}\mathcal{Q}e^{i\Delta}e^{i(ky-\omega t)}, & y > x \\ \mathcal{Q}e^{i(ky-\omega t)} + 2^{-1/2}\mathcal{Q}e^{i(\Delta+\mu)}e^{i(kx-\omega t)}, & y < x \end{cases}$$

where it is assumed that the electric fields are
polarized out of the page. Here $k = \omega/c$ is the
wave number, $\mathcal{Q}$ is a real constant determined
by one's choice of normalization, and the overall
phase shift Δ and the relative phase shift μ are
properties of the beam splitter. The relation
between the phase shifts the two modes suffer
at the beam splitter is dictated by the assumed
symmetries of the beam splitter—time-reversal
invariance and reflection symmetry through the
plane $x = -y$. (The further and unnecessary as-
sumption of reflection symmetry through the
plane $x = y$ was made in Ref. 11; this assumption
implies $\mu = \pi/2$.)

The other two modes of interest (modes 1^- and
2^-) are "out" modes (time reversed "in" modes).
Out modes are appropriate for constructing post-
collision wave packets. Modes 1^- and 2^- are the
out modes whose exiting plane waves propagate
along the x and y axes, respectively. The sym-
metries of the beam splitter allow one to relate
the electric fields of the out modes to those of
the in modes:

$$E_1^- = 2^{-1/2}e^{-i\Delta}(E_1^+ + e^{-i\mu}E_2^+),$$
$$E_2^- = 2^{-1/2}e^{-i\Delta}(E_2^+ - e^{i\mu}E_1^+).$$

$$\tag{2.13}$$

Now let the creation and annihilation operators
for modes 1^+ and 2^+ be denoted by $a_1^\dagger$, a_1 and $a_2^\dagger$,
a_2; similarly, for modes 1^- and 2^-, $b_1^\dagger$, b_1 and
$b_2^\dagger$, b_2. Equation (2.13) implies

$$b_1 = 2^{-1/2}e^{i\Delta}(a_1 + e^{i\mu}a_2),$$
$$b_2 = 2^{-1/2}e^{i\Delta}(a_2 - e^{-i\mu}a_1).$$

$$\tag{2.14}$$

The operator $\mathcal{P}$ that specifies the difference
between the momenta transferred to the end

masses is proportional to the difference between the number of photons in modes 1^- and 2^-:

$$\mathcal{P} \equiv (2b\hbar\omega/c)(b_2^\dagger b_2 - b_1^\dagger b_1)$$
$$= -(2b\hbar\omega/c)(e^{i\mu}a_1^\dagger a_2 + e^{-i\mu}a_2^\dagger a_1). \qquad (2.15)$$

Note that, when written in terms of operators for the in modes, $\mathcal{P}$ is clearly due solely to the interference of modes 1^+ and 2^+. This is merely a restatement of the fact, true classically, that the difference in the intensity in the two arms of an interferometer is produced solely by the interference of light coming from the two input ports.

Now assume the state of the electromagnetic field is

$$|\Psi\rangle = S_2(\zeta)D_1(\alpha)|0\rangle, \quad \alpha \text{ real}, \quad \zeta = -re^{-2i\mu}, \qquad (2.16)$$

where D_1 is the displacement operator for mode 1^+ and S_2 is the squeeze operator for mode 2^+ [see Eqs. (2.3) and (2.7)]. Mode 1^+ is in a coherent state with complex amplitude α (the choice of α real is merely a choice of phase for mode 1^+), and mode 2^+ is in a squeezed state with zero expected complex amplitude. Note that the squeeze factor r can be either positive or negative. The phase with which mode 2^+ is squeezed is chosen carefully so that, in the arms of the interferometer, the reduced-noise quadrature phase of mode 2^+ is either in phase or 90° out of phase with the coherent excitation of mode 1^+. The numbers of photons in modes 1^+ and 2^+ and their variances are given by

$$(N_1)_{\text{in}} = \langle a_1^\dagger a_1\rangle = \alpha^2 ,$$
$$(\Delta N_1)_{\text{in}}^2 = \alpha^2 ,$$
$$(N_2)_{\text{in}} = \langle a_2^\dagger a_2\rangle = \sinh^2 r , \qquad (2.17)$$
$$(\Delta N_2)_{\text{in}}^2 = 2\cosh^2 r \sinh^2 r$$

[cf. Eqs. (2.6) and (2.11)]. To relate to the case where the light has a finite duration τ, one uses the mean numbers of photons in the two modes to define a mean power P into the laser port and a mean power P_2 into the normally unused input port:

$$P = \hbar\omega\alpha^2/\tau , \qquad (2.18)$$
$$P_2 = \hbar\omega\sinh^2 r/\tau .$$

For reasonable values of r, P_2 is an extremely small power ($\hbar\omega/\tau \sim 2 \times 10^{-16}$ W).

It is now a simple matter, using Eqs. (2.4) and (2.8), to evaluate the expectation value and variance of $\mathcal{P}$:

$$\langle\mathcal{P}\rangle = 0 , \qquad (2.19a)$$
$$(\Delta\mathcal{P})^2 = (2b\hbar\omega/c)^2(\alpha^2 e^{2r} + \sinh^2 r) . \qquad (2.19b)$$

Both terms in Eq. (2.19b) come from the interference of modes 1^+ and 2^+—the first term from the superposition of the coherent excitation of mode 1^+ on the fluctuations in mode 2^+ and the second from the interference of the fluctuations in the two modes. There is *no* contribution to Eq. (2.19b) from the superposition of the coherent excitation of mode 1^+ on fluctuations in mode 1^+; these input power fluctuations perturb only the *sum* of the end masses' momenta and, therefore, do not affect the interferometer's performance. Equation (2.19b) also displays the effect of putting mode 2^+ in a squeezed state. In the arms of the interferometer one quadrature phase of mode 2^+ is in phase with the coherent excitation of mode 1^+—but with opposite sign in the two arms. This phase is entirely responsible for the first term in Eq. (2.19b). By attenuating or amplifying the noise in this phase, one can reduce ($r < 0$) or increase ($r > 0$) $\Delta\mathcal{P}$.

In a time τ the disturbance (2.19b) of the difference between the end masses' momenta perturbs z by an amount

$$(\Delta z)_{\text{rp}} \simeq (\Delta\mathcal{P})\tau/2m = (b\hbar\omega\tau/mc)(\alpha^2 e^{2r} + \sinh^2 r)^{1/2} .$$

$$(2.20)$$

This is the *radiation-pressure* (rp) *error* in z. Below, $(\Delta z)_{\text{rp}}$ is used in an analysis of the optimum sensitivity and optimum power.

Before going on to a consideration of the photon-counting error, it is perhaps useful to look in a more general way at the intensity correlation of the light in the two arms of the interferometer. The beam-splitter modes of Eqs. (2.12) and (2.13) are ideally suited to a discussion of a characteristic intensity-correlation experiment in quantum optics—an experiment of the type pioneered by Hanbury Brown and Twiss.[24,25] In such an experiment one counts the number of photons in the two beams emerging from a beam splitter and looks at the cross correlation of the number of counts. The quantity that characterizes this photon-number correlation is the *second-order coherence*,[12] which, for the simple case of two out modes considered here, is given by

$$g_{12}^{(2)} \equiv \frac{\langle b_1^\dagger b_1 b_2^\dagger b_2\rangle}{\langle b_1^\dagger b_1\rangle\langle b_2^\dagger b_2\rangle} . \qquad (2.21)$$

If $g_{12}^{(2)} > 1$, the intensities in the two output beams are correlated—a phenomenon known as photon bunching. If $g_{12}^{(2)} < 1$, the intensities are anti-correlated—a situation referred to as anti-bunching. Antibunching is generally considered to be an intrinsically quantum-mechanical property of light; a great deal of effort has gone into trying to produce and detect antibunched light.[26]

To see how squeezed states fit into this picture, I consider a more general state of the field than $|\Psi\rangle$. This state,

$$|\Psi'\rangle = S_2(\zeta_2)D_1(\alpha)S_1(r_1)|0\rangle,$$

$$\alpha \text{ and } r_1 \text{ real}, \quad \zeta_2 = -r_2 e^{-2i\mu}, \quad (2.22)$$

differs from $|\Psi\rangle$ in that mode 1^+ is in an excited *squeezed* state with complex amplitude α (S_1 is the squeeze operator for mode 1^+). The squeezing of mode 1^+ is of the sort depicted in Figs. 2(b) and 2(c).

Using Eqs. (2.14), (2.4), and (2.8), one can evaluate the second-order coherence of $|\Psi'\rangle$:

$$g^{(2)}_{12} = 1 + \frac{Q}{(\alpha^2 + \sinh^2 r_1 + \sinh^2 r_2)^2}, \quad (2.23a)$$

$$Q = \alpha^2 e^{-2r_1} - \alpha^2 e^{2r_2} + 2\cosh^2 r_1 \sinh^2 r_1$$

$$+ 2\cosh^2 r_2 \sinh^2 r_2$$

$$- (\sinh r_1 \cosh r_2 - \cosh r_1 \sinh r_2)^2. \quad (2.23b)$$

The terms in Q have simple physical interpretations: the first and second terms come from interference of the coherent excitation of mode 1^+ with the fluctuations in modes 1^+ and 2^+; the third and fourth terms come from the fluctuations in the two modes separately; and the last term comes from interference of the fluctuations in the two modes. The terms arising from each in mode separately (terms 1, 3, and 4) always make a positive (correlated) contribution to Q, whereas the interference terms (terms 2 and 5) always make a negative (anticorrelated) contribution.

Only one quadrature phase of each in mode is in phase with the coherent excitation of mode 1^+. These in-phase quadratures are responsible for the first two terms in Q. Thus, by squeezing the in modes to put more or less noise in the in-phase quadratures, one can make the light bunched ($Q > 0$) or antibunched ($Q < 0$). Rewriting Q in a different form makes it clear that only the first two terms in Q can lead to antibunching:

$$Q = -2\alpha^2 e^{r_2 - r_1} \sinh(r_1 + r_2)$$

$$+ \sinh^2(r_1 + r_2)[1 + 2\sinh^2(r_1 - r_2)]. \quad (2.24)$$

The pure-fluctuation terms in Q always make a net positive contribution.

It is useful now to look at some special cases of the above. The simplest is the case where mode 1^+ is in a coherent state ($r_1 = 0$) and mode 2^+ is in the vacuum state ($r_2 = 0$). Then one obtains the well-known result that $g^{(2)}_{12} = 1$. This lack of correlation results from the precise cancellation of the first two terms in Q [Eq. (2.23b)]; the correlated contribution due to

fluctuations in the input coherent state is canceled by the anticorrelated contribution due to vacuum fluctuations entering the other input port.

The second case is the one where mode 1^+ is in an excited squeezed state and mode 2^+ is again vacuum ($r_2 = 0$). The intensity correlations of this type of light have been investigated by several authors.[14,19,27,28] For this case Q takes the form

$$Q = \alpha^2(e^{-2r_1} - 1) + \sinh^2 r_1(1 + 2\sinh^2 r_1). \quad (2.25)$$

The light is bunched if one increases the noise in the quadrature phase of mode 1^+ that carries the coherent excitation [$r_1 < 0$; Fig. 2(c)]. It can be antibunched if one decreases the noise in that quadrature phase [$r_1 > 0$; Fig. 2(b)]. Note, however, that as one increases the value of r_1, the pure-fluctuation terms in Eq. (2.25) eventually dominate and the light becomes bunched. If $|\alpha| \gg 1$ this transition from antibunching to bunching occurs when $r_1 \simeq \frac{1}{4}\ln(8\alpha^2)$.

The last case is the one where mode 1^+ is in a coherent state ($r_1 = 0$), but mode 2^+ is in a squeezed state. Then Q takes the form

$$Q = \alpha^2(1 - e^{2r_2}) + \sinh^2 r_2(1 + 2\sinh^2 r_2). \quad (2.26)$$

This case is similar to the previous one. The output light is bunched if one decreases the noise in the quadrature phase of mode 2^+ that gives rise to the anticorrelated contribution in Eq. (2.26) ($r_2 < 0$). The output light can be antibunched if one increases the noise in that quadrature phase [$r_2 > 0$; it is antibunched light of this sort that increases the radiation-pressure error (2.20) in an interferometer]. As in the previous case, the light eventually becomes bunched as one increases r_2, the transition occurring at $r_2 \simeq \frac{1}{2}\ln(8\alpha^2)$ if $|\alpha| \gg 1$. That this case can produce antibunched light is perhaps not very surprising, because if one allows light to enter both input ports of a beam splitter, anticorrelation can be obtained using classical light. On the other hand, this case should not be dismissed too quickly, because the squeezed state of mode 2^+, with its zero expected complex amplitude, is certainly not like a classical radiation field.

The antibunched light discussed in this section is different from the antibunched light that has been produced and detected in a recent series of experiments.[29,30] In these experiments the goal has been to produce light that is closer to a photon-number eigenstate than a coherent state is. Such light is antibunched by virtue of its reduced amplitude fluctuations, which are purchased at the price of an ill-defined phase. For the case of a squeezed mode 1^+ ($r_2 = 0$, $r_1 > 0$), the light considered here is also antibunched because of de-

creased (correlated) amplitude fluctuations, and the phase is correspondingly less well defined than for a coherent state. For the case of a squeezed mode 2^+ ($r_1 = 0$, $r_2 > 0$), however, the antibunching is due to increased (anticorrelated) amplitude fluctuations, and the phases of the two output beams are better defined than for a coherent state. The difference between the light used in the current experiments and the light considered here could be observed using phase-sensitive detection of the two beams from the beam splitter.

3. Photon-counting error

For the case of ideal photodetectors, the photocount statistics of the photodetectors are the same as the photon statistics, so the photon-counting error can be determined simply by calculating the fluctuations in number of output photons. Just as for the case of radiation-pressure fluctuations, this calculation requires only four modes of the electromagnetic field, but now they must be modes for the entire interferometer ("interferometer modes").

The in modes of interest are again called modes 1^+ and 2^+, with mode 1^+ describing light incident from the input (laser) port and mode 2^+ describing light incident from the other input port. Outside the arms of the interferometer the electric fields of the two in modes have the forms

$$E_1^+ = \begin{cases} \mathcal{C}e^{i(kx-\omega t)} - i\mathcal{C}e^{i(\Phi-\mu)}\sin(\phi/2)e^{-i(kx+\omega t)}, & y > x \\ \mathcal{C}e^{i\Phi}\cos(\phi/2)e^{-i(ky+\omega t)}, & y < x \end{cases}$$

(2.27)

$$E_2^+ = \begin{cases} \mathcal{C}e^{i\Phi}\cos(\phi/2)e^{-i(kx+\omega t)}, & y > x \\ \mathcal{C}e^{i(ky-\omega t)} - i\mathcal{C}e^{i(\Phi+\mu)}\sin(\phi/2)e^{-i(ky+\omega t)}, & y < x \end{cases}$$

where $\mathcal{C}$ is a (real) normalization constant. The phases ϕ and Φ can be defined precisely as follows: let light enter the interferometer from the laser port, and consider the output light in the bottom output port of Fig. 3 ($-y$ direction); then ϕ is the phase difference between the light from the two arms, and Φ is the mean phase. The two phases are related to the (constant) positions of the end mirrors by

$$\phi = 2b\omega z/c + \pi - 2\mu , \qquad (2.28a)$$

$$\Phi = 2b\omega Z/c + \Phi_0 , \qquad (2.28b)$$

where $Z \equiv \frac{1}{2}(z_1 + z_2)$ and Φ_0 is a constant.

The two out modes, again called modes 1^- and 2^-, are the time reverses of the in modes. Mode

1^- is the time reverse of mode 1^+ and, therefore, describes light leaving the interferometer along the $-x$ axis. Mode 2^-, the time reverse of mode 2^+, describes light exiting along the $-y$ axis. The fields of the two sets of modes are related by

$$E_1^- = e^{-i\Phi}[ie^{i\mu}E_1^+\sin(\phi/2) + E_2^+\cos(\phi/2)],$$

(2.29)

$$E_2^- = e^{-i\Phi}[E_1^+\cos(\phi/2) + ie^{-i\mu}E_2^+\sin(\phi/2)].$$

The creation and annihilation operators for the interferometer in modes are denoted $a_1^\dagger$, a_1 and $a_2^\dagger$, a_2; similarly, for the interferometer out modes, $c_1^\dagger$, c_1 and $c_2^\dagger$, c_2. Equation (2.29) implies

$$c_1 = e^{i\Phi}[-ie^{-i\mu}a_1\sin(\phi/2) + a_2\cos(\phi/2)],$$

(2.30)

$$c_2 = e^{i\Phi}[a_1\cos(\phi/2) - ie^{i\mu}a_2\sin(\phi/2)].$$

The operators of interest are the photon-number operators for the two out modes and the difference between these two. These are given by

$$c_2^\dagger c_2 - c_1^\dagger c_1 = (a_1^\dagger a_1 - a_2^\dagger a_2)\cos\phi$$
$$- i\sin\phi(e^{i\mu}a_1^\dagger a_2 - e^{-i\mu}a_2^\dagger a_1),$$

(2.31)

$$c_1^\dagger c_1 = a_1^\dagger a_1\sin^2(\phi/2) + a_2^\dagger a_2\cos^2(\phi/2)$$
$$+ i\sin(\phi/2)\cos(\phi/2)(e^{i\mu}a_1^\dagger a_2 - e^{-i\mu}a_2^\dagger a_1) ,$$

(2.32)

where $c_2^\dagger c_2$ can be obtained from $c_1^\dagger c_1$ by the transformation $\phi \to \phi + \pi$.

Now assume, as before, that the electromagnetic field is in the state $|\Psi\rangle$ of Eq. (2.16). For this state the expectation values and variances of the operators (2.31) and (2.32), evaluated using Eqs. (2.4) and (2.8), are

$$n_{\text{out}} \equiv \langle c_2^\dagger c_2 - c_1^\dagger c_1 \rangle = \cos\phi(\alpha^2 - \sinh^2 r), \qquad (2.33a)$$

$$\Delta n_{\text{out}}^2 = \alpha^2\cos^2\phi + 2\cos^2\phi\cosh^2 r\sinh^2 r$$
$$+ \sin^2\phi(\alpha^2 e^{-2r} + \sinh^2 r) , \qquad (2.33b)$$

$$(N_1)_{\text{out}} \equiv \langle c_1^\dagger c_1 \rangle = \alpha^2\sin^2(\phi/2) + \cos^2(\phi/2)\sinh^2 r , \qquad (2.34a)$$

$$(\Delta N_1)_{\text{out}}^2 = \alpha^2\sin^4(\phi/2) + 2\cos^4(\phi/2)\cosh^2 r\sinh^2 r$$
$$+ \sin^2(\phi/2)\cos^2(\phi/2)(\alpha^2 e^{-2r} + \sinh^2 r) . \qquad (2.34b)$$

Equations (2.34) characterize the output (signal and noise) of an ideal photodetector in one of the output ports (mode 1^-), and Eqs. (2.33) characterize the differenced output of two ideal photode-

tectors, one in each output port.

Changes in z are detected by looking at changes in n_{out} or $(N_1)_{out}$. Taking the case of differenced photodetectors, one finds that a change δz produces a change

$$\delta n_{out} = -(2b\omega/c)\alpha^2 \sin\phi \, \delta z \qquad (2.35)$$

in n_{out}, where I assume $|\alpha| \gg |\sinh r|$ in order to neglect the second term in Eq. (2.33a), and where Eq. (2.28a) is used to convert ϕ to z. Using Eq. (2.35) to transform Δn_{out} into a corresponding error in z, one obtains a *photon-counting* (pc) *error*:

$$(\Delta z)_{pc} \simeq \frac{c}{2b\omega} \left(\frac{\cot^2\phi}{\alpha^2} + \frac{2\cot^2\phi \cosh^2 r \sinh^2 r}{\alpha^4} \right.$$
$$\left. + \frac{e^{-2r}}{\alpha^2} + \frac{\sinh^2 r}{\alpha^4} \right)^{1/2} . \qquad (2.36)$$

For the case of a single photodetector [Eqs. (2.34)], a similar calculation yields the following *photon-counting error*:

$$(\Delta z)_{pc} \simeq \frac{c}{2b\omega} \left[\frac{\tan^2(\phi/2)}{\alpha^2} + \frac{2\cot^2(\phi/2)\cosh^2 r \sinh^2 r}{\alpha^4} \right.$$
$$\left. + \frac{e^{-2r}}{\alpha^2} + \frac{\sinh^2 r}{\alpha^4} \right]^{1/2} , \qquad (2.37)$$

where it is necessary to assume $|\alpha| \gg |\cot(\phi/2) \sinh r|$ in order to neglect the second term in Eq. (2.34a).

The terms in Eqs. (2.36) and (2.37) [or, alternatively, in Eqs. (2.33b) and (2.34b)] can be interpreted in ways familiar from the earlier discussions of $\Delta\mathcal{P}$ and Q. The first term in both equations comes from fluctuations in mode 1^+ superposed on the coherent excitation of mode 1^+ (input power fluctuations), the second term comes from fluctuations in mode 2^+, and the last two terms come from the interference of modes 1^+ and 2^+. For the case of differenced photodetectors [Eq. (2.36)], both of the first two terms can be made zero by operating at an appropriate place in the fringe pattern ($\cos\phi = 0$); hence, input power fluctuations can be made irrelevant. For a single photodetector [Eq. (2.37)], the contribution from input power fluctuations can be made negligible by operating near a null fringe [$\sin(\phi/2) \simeq 0$], and as long as $|\alpha| \gg |\cot(\phi/2)e^r \cosh r \sinh r|$, the second term in Eq. (2.37) is also negligible compared to the interference terms. Thus, in either case, one can arrange that the dominant contribution to the photon-counting error comes from the interference of modes 1^+ and 2^+; since the interference terms in Eqs. (2.36) and (2.37) are independent of position in the fringe pattern (i.e., independent of ϕ), they make the truly *unavoidable* contribution to the photon-counting error.

The third term in Eqs. (2.36) and (2.37) displays a result of a now-familiar sort: only one quadrature phase of mode 2^+ superposes on the coherent excitation of mode 1^+ to contribute to the photon-counting error. This quadrature phase is not the one that makes the same sort of contribution to the radiation-pressure error [cf. third term in Eqs. (2.36) and (2.37) and first term in Eq. (2.20)]. Consequently, squeezing mode 2^+ can reduce the photon-counting error while increasing the radiation-pressure error ($r > 0$), or vice versa ($r < 0$).

4. Optimum sensitivity and optimum power

The objective now is to investigate what happens to the interferometer's optimum sensitivity and optimum power as one squeezes mode 2^+. For the case of differenced photodetectors operating at $\cos\phi = 0$, the photon-counting error (2.36) and the radiation-pressure error (2.20) have the forms

$$(\Delta z)_{pc} \simeq (c/2b\omega)|\alpha|^{-1}e^{-r} , \qquad (2.38)$$

$$(\Delta z)_{rp} \simeq (b\hbar\omega\tau/mc)|\alpha|e^r . \qquad (2.39)$$

Here I assume that α^2 is large enough so that the last term in both Eq. (2.20) and Eq. (2.36) can be neglected—i.e., I assume that $|\alpha| \gg \sinh^2 r$, which is equivalent to $P_2 \ll (P\hbar\omega/\tau)^{1/2}$ [see Eq. (2.18)]. The total error is $\Delta z = [(\Delta z)_{pc}^2 + (\Delta z)_{rp}^2]^{1/2}$. If one minimizes the total error with respect to α^2, one finds a minimum error

$$(\Delta z)_{opt} \simeq (\hbar\tau/m)^{1/2} \simeq (\Delta z)_{SQL} \qquad (2.40)$$

[see Eq. (1.1)] and an optimum value for α^2,

$$\alpha_{opt}^2 \simeq \alpha_0^2 e^{-2r} , \quad \alpha_0^2 \equiv \tfrac{1}{2}(mc^2/\hbar\omega)(1/\omega\tau)(1/b^2) . \qquad (2.41)$$

The quantity α_{opt}^2 is the optimum number of photons in mode 1^+ [see Eq. (2.17)], and it translates into an optimum input power

$$P_{opt} \simeq P_0 e^{-2r} , \qquad (2.42)$$

where $P_0 \equiv \hbar\omega\alpha_0^2/\tau$ is the optimum power for a standard ($r = 0$) interferometer [Eq. (1.2)]. For the fiducial parameters, $\alpha_0^2 \sim 4 \times 10^{19}$ and $P_0 \sim 8 \times 10^3$ W.

Equation (2.42) displays the desired result: the optimum power can be adjusted by squeezing the vacuum before it can enter the normally unused input port. There are, however, limits to the validity of Eqs. (2.41) and (2.42)—limits imposed by the validity condition, $|\alpha| \gg \sinh^2 r$, for Eqs. (2.38) and (2.39). What happens, for example, if the squeeze factor r becomes so large that α_{opt} violates this condition? The answer is contained

in the exact equation for the photon-counting error [Eq. (2.36)]. As the squeeze factor is increased past a value $r_{max} \sim \frac{1}{3} \ln \alpha_0$, the last term in Eq. (2.36) begins to dominate the optimum sensitivity. For $r \gtrsim r_{max}$ the optimum sensitivity becomes rapidly worse than the standard quantum limit. As a result, the maximum useful value of r for this case of differenced photodetectors is r_{max}, which corresponds to a minimum optimum power $(P_{opt})_{min} \sim (P_0{}^2 \hbar \omega / \tau)^{1/3} [(\alpha_{opt}{}^2)_{min} \sim \alpha_0{}^{4/3}]$ and a power into the other port $P_2 \sim [P_0(\hbar \omega / \tau)^2]^{1/3}$ [Eq. (2.18)].

For the case of a single photodetector [Eq. (2.37)] operated near a null fringe [$\sin(\phi/2) \simeq 0$], one obtains the same results (2.38)–(2.42), but with more stringent validity conditions, $|\alpha| \gg \sinh^2 r$ and $|\alpha| \gg e^{2r} \sinh^2 r$, because of the second term in Eq. (2.37). These more stringent validity conditions mean that the optimum power cannot be reduced as much as in the case of differenced photodetectors (see, however, the discussion at the end of Sec. III).

One interesting question not investigated in the above analysis is whether there is some reason to squeeze the light in mode 1^+. Doing so can, for example, reduce the size of the first term in Eqs. (2.36) and (2.37), but there is little point in doing this, because this term can be made negligible by operating at an appropriate place in the fringe pattern. There is, however, another reason for squeezing the input laser light. Recall that, for the case of differenced photodetectors, the term that limits the reduction of the optimum power is the last term in the photon-counting error (2.36)—a term that arises from the interference of fluctuations in modes 1^+ and 2^+. For $r \gg 1$ the noise in mode 2^+ is concentrated in one quadrature phase, so one can reduce the size of this term by squeezing mode 1^+ with appropriate phase. In doing so, however, one inevitably increases the term of the same type in the radiation-pressure error [second term in Eq. (2.20)]. In particular, if one puts the field in the state $|\Psi'\rangle$ of Eq. (2.22) with $r_2 = -r_1 = r$ (squeezed light into both input ports), one finds that the last term in Eq. (2.36) disappears, but the last term in Eq. (2.20) becomes $\sinh^2 2r$ rather than $\sinh^2 r$. The result is a minimum optimum power

$$(P_{opt})_{min} \sim (P_0 \hbar \omega / \tau)^{1/2} \sim P_2 \qquad (2.43)$$

[$r_{max} \sim \frac{1}{2} \ln \alpha_0$, $(\alpha_{opt}{}^2)_{min} \sim \alpha_0$]. Equations (2.18) and (2.42) imply that, for $r \gg 1$, $P_{opt} P_2 \sim P_0 \hbar \omega / \tau$, so Eq. (2.43) is the best one can do in reducing the total power $P_{opt} + P_2$ required to run an interferometer at the standard quantum limit.

Squeezing the input laser light finds another application in an interferometer that measures Z

$= \frac{1}{2}(z_1 + z_2)$ rather than z. The intensity in an interferometer's output ports is determined by z, but the phase of the output is determined by Z. A standard interferometer, in which one monitors the output intensity, is sensitive only to changes in z, but an interferometer in which one monitored the output light using phase-sensitive detection would be sensitive to changes in Z. For the case of a coherent state in mode 1^+ and vacuum in mode 2^+, a Z interferometer would have an optimum sensitivity $(\Delta Z)_{opt} \simeq (\hbar \tau / m)^{1/2}$ and an optimum power P_0. By squeezing the light in mode 1^+, one could adjust the optimum power just as in Eq. (2.42).

III. PRACTICAL CONSIDERATIONS RELATED TO SQUEEZED-STATE TECHNIQUE

In this section I turn from the abstract analysis of Sec. II to somewhat more practical matters related to implementing the squeezed-state technique. In particular, I focus on the situation relevant for real interferometers, which are limited by photon-counting statistics. The strain sensitivity of such an interferometer is given by

$$\frac{(\Delta z)_{pc}}{l} \simeq \frac{c}{2b\omega l} \frac{e^{-r}}{|\alpha|} = \frac{c}{2b\omega l} \left(\frac{\hbar \omega}{P\tau}\right)^{1/2} e^{-r}$$

$$= \frac{1}{\omega \tau_s} \left(\frac{\hbar \omega}{P\tau}\right)^{1/2} e^{-r} \qquad (3.1)$$

[Eqs. (2.38) and (2.18)]. For a given measurement time τ, one can improve the strain sensitivity by increasing b, ω, l, P, or r. Thus, the squeezed-state technique provides an additional option for improving the strain sensitivity. The availability of this option might be important, because changes in the interferometer's other parameters might be precluded by practical limitations—e.g., unavailability of cw lasers of higher power or higher frequency, unavailability of optical components to handle higher powers or higher frequencies, or limitations on the size of high-quality mirrors.

There is one situation in which the squeezed-state technique might be especially important. The improvement in strain sensitivity afforded by increasing the number of bounces b or the baseline l is limited by the condition that the storage time $\tau_s = 2bl/c$ be less than the measurement time τ. For $\tau_s > \tau$ the sensitivity does not improve beyond the value attained at $\tau_s \simeq \tau$; this limits the strain sensitivity of a standard ($r = 0$) interferometer to $(\Delta z)_{pc}/l \simeq (\hbar / P \omega \tau^3)^{1/2}$. The greatest potential usefulness of the squeezed-state technique probably lies in its ability to improve the sensitivity of an interferometer for which $\tau_s \simeq \tau$, without increasing the input power P.

In considering the design of a squeezed-state interferometer, the first question to be addressed is how to generate the required squeezed states. One way of generating squeezed states is to use a degenerate parametric amplifier. An *optical parametric amplifier*[31] is an optical component in which one pumps a nonlinear medium, which has a nonvanishing second-order nonlinear suscept-ibility, with an electromagnetic wave whose angular frequency is denoted ω_p. The nonlinearity of the medium couples this pump wave to two other wave modes, called the signal and the idler, whose frequencies ω_s and ω_i satisfy $\omega_s + \omega_i = \omega_p$. If the wave vectors of the three waves in the med-ium satisfy, or nearly satisfy, $\vec{k}_s + \vec{k}_i = \vec{k}_p$ (phase-matching condition), then the signal and idler are amplified (neglecting losses) as they propagate through the medium. A *degenerate parametric amplifier* is a parametric amplifier for which the signal and idler coincide ($\omega_s = \omega_i = \frac{1}{2}\omega_p$, $\vec{k}_s = \vec{k}_i = \frac{1}{2}\vec{k}_p$).

A degenerate parametric amplifier is a phase-sensitive device: it amplifies one quadrature phase of the signal mode, and it attenuates the other. Takahasi[32] was the first to point out that this behavior applies to the quantum-mechanical fluctuations in the mode. He considered a simple model of a degenerate parametric amplifier, a harmonic oscillator (the signal mode) whose spring constant is modulated classically (the pump modu-lation) at twice the oscillator's frequency, and he showed that an initial coherent state for the os-cillator is transformed into a state whose uncer-tainties in the two quadrature phases are unequal. Since Takahasi's work, there have been several quantum-mechanical analyses[14, 27, 33-35] of the light generated by an optical degenerate parametric amplifier. These analyses vary in complexity, some including the effects of losses in the non-linear medium[33, 35] and the effects of jitter in the amplitude and phase of the pump.[34]

The basic conclusion to be drawn from these analyses is that an ideal degenerate parametric amplifier generates squeezed states.[14, 27] Specif-ically, the state of the signal mode at the output of a degenerate parametric amplifier is obtained by applying the squeeze operator (2.7) to the state at the input. The phase of the squeezing [θ in Eq. (2.7)] is determined by the phase of the pump, and the squeeze factor r can be read off the results of a classical analysis[31]:

$$r = \left(\frac{4\pi\omega_s L}{cn_s}\right)d\,|E_p|$$

$$= \left(\frac{4\pi\omega_s L}{cn_s}\right)d\left(\frac{8\pi P_p}{cn_p A}\right)^{1/2} \quad \text{(cgs units)}. \quad (3.2)$$

Here I assume there is perfect phase matching at

degeneracy, and I use the notation of Ref. 31: d is the effective nonlinear susceptibility, E_p is the amplitude of the pump wave's electric field, L is the length over which the interaction takes place in the nonlinear medium, and n_s and n_p are the values of the index of refraction at the signal and pump frequencies. In the second part of Eq. (3.2) I have converted the pump electric field into a pump power P_p distributed over an area A.

The best nonlinear optical media have $d/n^{3/2}$ $\sim 10^{-8}$ in cgs units.[31] Thus, for a pump power $P_p \sim 100$ mW $= 10^6$ erg sec^{-1}, a beam area $A \sim 3$ $\times 10^{-2}$ cm^2, an interaction length $L \sim 10$ cm, and a signal frequency $\omega_s \sim 4 \times 10^{15}$ rad sec^{-1}, the squeeze factor is $r \sim 0.03$. This does not look very encouraging, and one must remember that the es-timate is overly optimistic because losses in the medium have been neglected. There is, however, a way to increase the achievable squeeze factor. If the single-pass loss through the medium does not exceed the single-pass gain, one can increase the squeeze factor (gain) by enclosing the medium in an optical cavity that resonates at the signal frequency. This increases the effective interac-tion length, because the signal wave passes through the nonlinear medium many times before it leaves the cavity. The resulting device is called an *optical parametric oscillator*.[31] For pump powers of 10–100 mW, parametric oscilla-tors at optical frequencies have achieved a signal-mode output of a few milliwatts in a bandwidth of about an angstrom[31]; this corresponds to a squeeze factor $e^r \sim 200$ ($r \sim 5$). The bandwidth here is huge compared to that necessary in a gravita-tional-wave interferometer; nonetheless, these results hint at the possibility of achieving reason-able squeeze factors.

Even given a reasonable squeeze factor, there are still stringent demands on the operation of the degenerate parametric amplifier in an inter-ferometer. The critical demands are that the amplifier be pumped at exactly twice the frequen-cy of the laser ($\omega_p = 2\omega$) and that the pumping be done with just the right phase so that the vacuum is squeezed with a phase that is properly matched to the phase of the laser [see Eq. (2.16)]. To satisfy these demands in practice, one would probably extract a small fraction of the laser light at a beam splitter, run this light through a fre-quency doubler, and then use the doubled light (with just the right phase) to pump a degenerate parametric amplifier located in the normally un-used input port. This scheme is shown in Fig. 4. If the nonlinear medium is pumped at exactly twice the laser frequency, it is *not* necessary that the amplifier operate precisely at degener-acy. If it operates a small distance from degen-

eracy, then it produces two output waves, a signal and an idler, whose frequencies satisfy $\omega_s + \omega_i = \omega_p = 2\omega$; the fluctuations in these two waves are correlated in just such a way that their superposition mimics the behavior of a squeezed state at frequency ω.

There are a host of practical problems to be faced in implementing the squeezed-state technique using a degenerate parametric amplifier. Nonetheless, the brief discussion given here is perhaps sufficiently encouraging to motivate further investigation of the idea.

Degenerate parametric amplification is not the only optical process that generates squeezed states. Any phase-sensitive nonlinear process is a good candidate. For example, Yuen and Shapiro[36] have pointed out that a degenerate four-wave mixer generates output waves that can produce squeezed states when they are combined at a beam splitter. Four-wave mixers are now being vigorously developed because of their ability to produce phase-conjugated (time-reversed) light.[37] Yuen[18, 19] has also suggested that an ideal two-photon laser would produce squeezed states.

The losses in real mirrors are likely to impose the most severe practical limitation on the usefulness of the squeezed-state technique. Losses destroy the crucial feature of the technique—the

reduced noise in one of the two quadrature phases of mode 2^+. One can estimate the effect of losses from the following argument. Consider a nearly monochromatic beam of light bouncing back and forth between mirrors of reflectivity $\mathfrak{R}$. If one identifies $\mathfrak{R}$ as the probability that a given photon is reflected, then a simple "random-walk" argument yields the mean and variance of the number of photons in the beam after q reflections:

$$N_q = N_0 \mathfrak{R}^q , \tag{3.3a}$$

$$(\Delta N)_q^2 = (\Delta N)_0^2 \mathfrak{R}^{2q} + N_0 \mathfrak{R}^q (1 - \mathfrak{R}^q) . \tag{3.3b}$$

Here the subscript 0 designates the initial values. Since reflection is a linear process, Eqs. (3.3) suggest that, after q reflections, the X_1 and X_2 of the light beam have the following variances:

$$(\Delta X_1)_q^2 = (\Delta X_1)_0^2 \mathfrak{R}^q + \tfrac{1}{4} (1 - \mathfrak{R}^q) ,$$

$$(\Delta X_2)_q^2 = (\Delta X_2)_0^2 \mathfrak{R}^q + \tfrac{1}{4} (1 - \mathfrak{R}^q) . \tag{3.4}$$

Equations (3.3) and (3.4) have the same form as the equations for a damped harmonic oscillator in contact with a heat reservoir at zero temperature. The first term in Eqs. (3.3b) and (3.4) represents the damping of the initial fluctuations, and the second term represents the fluctuations added
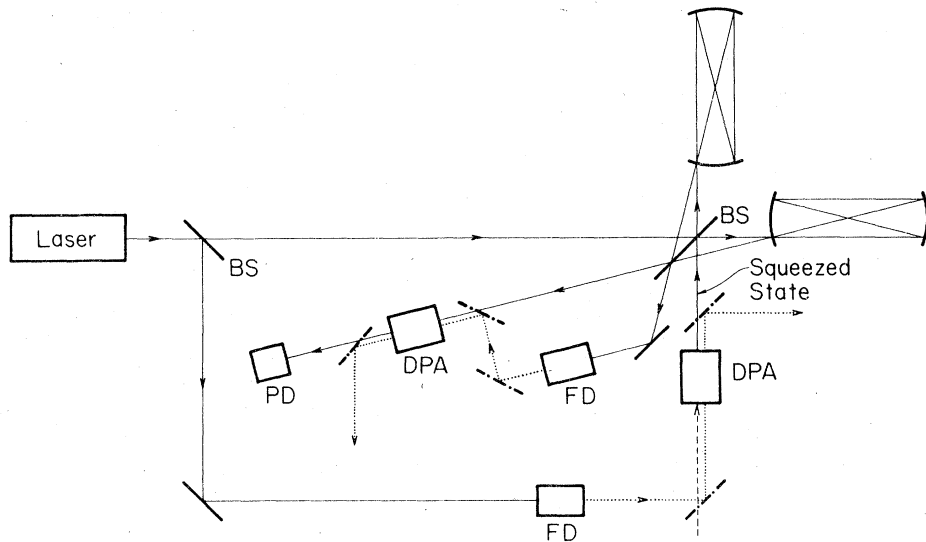

FIG. 4. Squeezed-state interferometer (abbreviations: BS = beam splitter; FD = frequency doubler; DPA = degenerate parametric amplifier; PD = photodetector). The crucial feature of the squeezed-state technique is the DPA located in the normally unused input port. This DPA takes the vacuum fluctuations incident on it (dashed arrow) and produces a squeezed state. To pump the DPA, one uses light that is extracted from the laser beam at a beam splitter and then doubled in frequency. There is another DPA in one of the output ports. This output DPA squeezes the light in that port, which is near a null in the fringe pattern, and thereby matches the noise in the light to the shot noise in an inefficient PD. The output DPA is pumped by frequency-doubled light from the other output port. The laser operates at frequency ω. Light beams at frequency ω are drawn with thin lines, and the components for handling them are drawn with heavy lines. The pump beams at frequency 2ω are drawn with dotted lines, and the mirrors for routing them are drawn with heavy, broken lines. These mirrors are assumed to transmit at frequency ω.

due to losses. The added fluctuations appear with random phase. Thus, an initial coherent state $[(\Delta X_1)_0 = (\Delta X_2)_0 = \frac{1}{2}, \ (\Delta N)_0{}^2 = N_0]$ remains coherent as its mean amplitude damps away. An initial squeezed state, however, loses its squeezed nature; the losses randomize the phase of its fluctuations, and its initial error ellipse becomes round.

In a squeezed-state interferometer, the added random-phase noise must be small enough so that it does not greatly increase the fluctuations in the low-noise quadrature phase of mode 2^+. This requirement suggests that the number of bounces b must satisfy

$$b \lesssim b_0 e^{-2r} \equiv e^{-2r} / (1 - \mathcal{R}) \tag{3.5}$$

[Eqs. (2.11), (2.16), and (3.4)], where I use the fact that the total number of reflections in each arm of the interferometer is $q = 2b - 1$, and where $b_0 \equiv (1 - \mathcal{R})^{-1}$ is the optimum number of bounces in a standard $(r = 0)$ interferometer.[6]

Equation (3.5) is a severe restriction. It implies that the squeezed-state technique can be used only if the interferometer is not limited by mirror losses (i.e., only if $b < b_0$). At the beginning of this section it was remarked that the most likely application of the squeezed-state technique is to interferometers whose number of bounces and baseline are large enough so that $\tau_s \simeq \tau$. The mirror-loss restriction (3.5) means that the technique can be used in this case only if $2b_0 l/c > \tau$— i.e., only if b_0 bounces correspond to a storage time longer than the desired measurement time (for $l \sim 1$ km and $\mathcal{R} \simeq 0.999$, $2b_0 l/c \sim 7 \times 10^{-3}$ sec). Thus, the potential usefulness of the squeezed-state technique is restricted to the case of a long baseline, high-reflectivity mirrors, and a short measurement time.

It is perhaps useful to emphasize the situation in which the squeezed-state technique is likely to become useful. Consider an interferometer operating with b_0 bounces and a measurement time τ. The interferometer's strain sensitivity can be improved by increasing its baseline, but this improvement continues only until $l \simeq c\tau/2b_0$, at which point the strain sensitivity is approximately $(\hbar/P\omega\tau^3)^{1/2}$. A further increase in length does not improve the strain sensitivity—unless one applies the squeezed-state technique as one decreases the number of bounces. Use of the squeezed-state technique allows the strain sensitivity to improve as $(\Delta z)_{pc}/l \simeq (\hbar/P\omega\tau^3)^{1/2}(c\tau/2b_0 l)^{1/2}$ for $l \gtrsim c\tau/2b_0$ [Eqs. (3.1) and (3.5)].

The analysis in Sec. II assumed ideal photodetectors—a case for which the photocount statistics at the output of the photodetectors coincide with the photon statistics of the light incident

on the photodetectors. If a photodetector has a quantum efficiency ξ less than one, then the photocount statistics are a combination of the photon statistics and the shot noise in the photodetector. How does the shot noise change the previously obtained photon-counting error? For the case of a single photodetector in one of the output ports [Eq. (2.34)], the mean and variance of the number of photons counted by the photodetector are given by[38]

$$N_{pd} = \xi (N_1)_{out} \ , \tag{3.6a}$$

$$\Delta N_{pd}{}^2 = \xi^2 (\Delta N_1)_{out}{}^2 + \xi(1 - \xi)(N_1)_{out} \ , \tag{3.6b}$$

where $(N_1)_{out}$ and $(\Delta N_1)_{out}$ are the mean and variance due to the photon statistics alone [Eqs. (2.34)]. The second term in (3.6b) is the shot-noise contribution. Using the same procedure as in Sec. III B 3, one can convert ΔN_{pd} into a photon-counting error,

$$(\Delta z)_{pc} \simeq \frac{c}{2b\omega} \left[\frac{\tan^2(\phi/2)}{\alpha^2} + \frac{e^{-2r}}{\alpha^2} \right.$$
$$\left. + \frac{1 - \xi}{\alpha^2 \xi \cos^2(\phi/2)} \right]^{1/2} . \tag{3.7}$$

Here I retain only the terms that dominate when $|\alpha|$ is sufficiently large. Near a null the first term in Eq. (3.7) is negligible, but the shot-noise contribution completely swamps the remaining photon-statistics term unless $1 - \xi \lesssim \xi e^{-2r}$. If the squeezed-state technique is to significantly improve the sensitivity, this requirement demands extraordinarily efficient photodetectors.

There is an alternative approach that avoids the requirement for high-efficiency photodetectors. The light emerging from the interferometer has an excellent signal-to-noise ratio near a null by virtue of its low noise in the quadrature phase that carries the signal. The photodetector ruins this good signal-to-noise ratio, because its shot noise is much larger than the noise in the light. To overcome this difficulty, one would like to amplify both the light signal and the noise in phase with the signal while keeping their ratio constant, thereby matching the noise in the light to the shot noise. This is precisely what would happen if one squeezed the output light before it reached the photodetector. The squeezing could be done by a degenerate parametric amplifier located in the appropriate output port (see Fig. 4).

Formally, the squeezing is described by introducing new creation and annihilation operators $\bar{c}_1^\dagger, \bar{c}_1$. These operators characterize the light emerging from the degenerate parametric amplifier, and they are related to the operators for interferometer mode 1^- by

$$\bar{c}_1 \equiv S_{c_1}^\dagger(\bar{\xi})c_1 S_{c_1}(\bar{\xi})$$

$$= c_1\cosh r - c_1^\dagger e^{2i(\Phi-\mu)}\sinh r, \quad \bar{\xi} = re^{2i(\Phi-\mu)}.$$

$$(3.8)$$

Here S_{c_1} is the squeeze operator for mode 1^-, and Eq. (2.8) is used to transform c_1. Note that the squeeze factor here is the same as the one used previously, and that the phase of the squeezing is carefully matched to the phase of the output light in mode 1^- [see Eqs. (2.28b) and (2.30)].

The mean and variance of the number of photons emerging from the degenerate parametric amplifier is obtained by evaluating the expectation value and variance of $\bar{c}_1^\dagger \bar{c}_1$ in the state $|\Psi\rangle$ of Eq. (2.16). Using Eqs. (3.8), (2.30), (2.4), and (2.8), one finds that

$$(\bar{N}_1)_{\text{out}} \equiv \langle \bar{c}_1^\dagger \bar{c}_1 \rangle = \sin^2(\phi/2)(\alpha^2 e^{2r} + \sinh^2 r),$$
$$(3.9a)$$

$$(\Delta\bar{N}_1)_{\text{out}}^2 = \sin^4(\phi/2)(\alpha^2 e^{4r} + 2\cosh^2 r \sinh^2 r)$$

$$+ \sin^2(\phi/2)\cos^2(\phi/2)(\alpha^2 e^{2r} + \sinh^2 r).$$
$$(3.9b)$$

These equations now replace Eqs. (2.34); they characterize the light incident on the photodetector. The disadvantage of this approach is revealed by Eq. (3.9a): unless one operates very close to a null fringe $[|\sin(\phi/2)| \ll e^{-r}]$, the power out of the degenerate parametric amplifier becomes comparable to or larger than the input power P—a situation clearly inconsistent with the operation of the parametric amplifier and with the desire to reduce the total power requirements. It is worth noting as a matter of principle that Eq. (3.9b), unlike Eq. (2.34b), imposes no restriction on the reduction of the optimum power. Thus, by using a degenerate parametric amplifier at the output, one can in principle achieve with a single photodetector the minimum total power of Eq. (2.43).

One can now obtain the mean and variance of the number of photons counted by the photodetector by applying Eqs. (3.6) to Eqs. (3.9). These results are then converted in the usual way into a photon-counting error in z:

$$(\Delta z)_{\text{pc}} \approx \frac{c}{2b\omega}\left\{ \frac{\tan^2(\phi/2)}{\alpha^2} + \frac{e^{-2r}}{\alpha^2}\left[1 + \frac{1-\xi}{\xi\cos^2(\phi/2)}\right]\right\}^{1/2}$$

$$\approx (c/2b\omega)\,\xi^{-1/2}\,|\alpha|^{-1}e^{-r} \quad \text{for } \sin(\phi/2) \approx 0.$$

$$(3.10)$$

Here I again retain only the terms that dominate

when $|\alpha|$ is large. Equation (3.10) explicitly demonstrates that insertion of a degenerate parametric amplifier into the output port allows one to use an inefficient photodetector without a significant increase in the photon-counting error [cf. Eqs. (3.10) and (2.38)].

To make this approach work, one must find a way to pump the degenerate parametric amplifier. The pump must have just the right phase relative to the phase of the output light in interferometer mode 1^-, to ensure that the squeezing of the output light occurs with the right phase. There is only one available beam of light that carries the necessary phase information, and that is the light in the other output port (interferometer mode 2^-). Since one wants to work very close to a null, there is plenty of power available in the other output port. One would take the light in the other output port, double its frequency, and then use the doubled light to pump the degenerate parametric amplifier in the output port. This approach is sketched in Fig. 4.

IV. CONCLUSION

The squeezed-state technique outlined in this paper will not be easy to implement. A refuge from criticism that the technique is difficult can be found by retreating behind the position that the entire task of detecting gravitational radiation is exceedingly difficult. Difficult or not, the squeezed-state technique might turn out at some stage to be the only way to improve the sensitivity of interferometers designed to detect gravitational waves. As interferometers are made longer, their strain sensitivity will eventually be limited by the photon-counting error for the case of a storage time approximately equal to the desired measurement time. Further improvements in sensitivity would then await an increase in laser power or implementation of the squeezed-state technique. Experimenters might then be forced to learn how to very gently squeeze the vacuum before it can contaminate the light in their interferometers.

[1] For reviews of efforts to detect gravitational waves and of theoretical estimates of gravitational-wave strengths, see K. S. Thorne, Rev. Mod. Phys. **52**, 285 (1980) and references cited therein; see also the chapters by R. Weiss and by R. Epstein and J. P. A. Clark, in *Sources of Gravitational Radiation*, edited by L. Smarr (Cambridge University Press, Cambridge, 1979).

[2] C. M. Caves, K. S. Thorne, R. W. P. Drever, V. D. Sandberg, and M. Zimmermann, Rev. Mod. Phys. **52**, 341 (1980).

[3] R. L. Forward, Phys. Rev. D **17**, 379 (1978).

[4] H. Billing, K. Maischberger, A. Rüdiger, R. Schilling, L. Schnupp, and W. Winkler, J. Phys. E **12**, 1043 (1979).

[5] R. W. P. Drever, J. Hough, W. A. Edelstein, J. R. Pugh, and W. Martin, in *Experimental Gravitation*, proceedings of a meeting held at Pavia, Italy, 1976, edited by B. Bertotti (Accademia Nazionale dei Lincei, Rome, 1977), p. 365.

[6] R. Weiss, in *Sources of Gravitational Radiation*, edited by L. Smarr (Cambridge University Press, Cambridge, 1979), p. 7.

[7] V. B. Braginsky and Yu. I. Vorontsov, Usp. Fiz. Nauk **114**, 41 (1974) [Sov. Phys.—Usp. **17**, 644 (1975)].

[8] R. Weiss, Quarterly Progress Report No. 105, Research Laboratory Electronics, MIT, 1972 (unpublished).

[9] W. Winkler, in *Experimental Gravitation*, proceedings of a meeting held at Pavia, Italy, 1976, edited by B. Bertotti (Accademia Nazionale dei Lincei, Rome, 1977), p. 351.

[10] W. A. Edelstein, J. Hough, J. R. Pugh, and W. Martin, J. Phys. E **11**, 710 (1978).

[11] C. M. Caves, Phys. Rev. Lett. **45**, 75 (1980).

[12] R. J. Glauber, Phys. Rev. **131**, 2766 (1963).

[13] D. Stoler, Phys. Rev. D **1**, 3217 (1970).

[14] E. Y. C. Lu, Lett. Nuovo Cimento **3**, 585 (1972).

[15] J. N. Hollenhorst, Phys. Rev. D **19**, 1669 (1979).

[16] D. Stoler, Phys. Rev. D **4**, 1925 (1971).

[17] E. Y. C. Lu, Lett. Nuovo Cimento **2**, 1241 (1971).

[18] H. P. Yuen, Phys. Lett. **51A**, 1 (1975).

[19] H. P. Yuen, Phys. Rev. A **13**, 2226 (1976).

[20] H. P. Yuen and J. H. Shapiro, IEEE Trans. Inf. Theory IT-24, 657 (1978).

[21] J. H. Shapiro, H. P. Yuen, and J. A. Machado Mata, IEEE Trans. Inf. Theory IT-25, 179 (1979).

[22] H. P. Yuen and J. H. Shapiro, IEEE Trans. Inf. Theory IT-26, 78 (1980).

[23] W. G. Unruh has sketched a procedure for doing a complete analysis of a standard interferometer (no squeezed states); see the chapter by Unruh in *Gravitational Radiation, Collapsed Objects, and Exact Solutions*, proceedings of the Einstein Centenary Summer School, Perth, Australia, 1979, edited by C. Edwards (Springer, Berlin, 1980), p. 385.

[24] R. Hanbury Brown and R. Q. Twiss, Nature **177**, 27 (1956).

[25] R. Hanbury Brown and R. Q. Twiss, Proc. R. Soc. London **A243**, 291 (1958).

[26] For a review of the theory of bunched and antibunched light and of the efforts to detect antibunching, see R. Loudon, Rep. Prog. Phys. **43**, 913 (1980), or D. F. Walls, Nature **280**, 451 (1979).

[27] D. Stoler, Phys. Rev. Lett. **33**, 1397 (1974).

[28] C. W. Helstrom, Opt. Commun. **28**, 363 (1979).

[29] H. J. Kimble, M. Dagenais, and L. Mandel, Phys. Rev. Lett. **39**, 691 (1977).

[30] M. Dagenais and L. Mandel, Phys. Rev. A **18**, 2217 (1978).

[31] A review of optical parametric amplifiers and parametric oscillators is given by R. G. Smith, in *Laser Handbook*, edited by F. T. Arecchi and E. O. Schulz-Dubois (North-Holland, Amsterdam, 1972), Vol. I, p. 837.

[32] H. Takahasi, Adv. Commun. Syst. **1**, 227 (1965), especially Sec. XI.

[33] M. T. Raiford, Phys. Rev. A **2**, 1541 (1970).

[34] M. T. Raiford, Phys. Rev. A **9**, 2060 (1974).

[35] L. Mišta, V. Peřinová, J. Peřina, and Z. Braunerová, Acta Phys. Pol. A **51**, 739 (1977).

[36] H. P. Yuen and J. H. Shapiro, Opt. Lett. **4**, 334 (1979).

[37] J. AuYeung and A. Yariv, *Laser Spectroscopy IV*, edited by H. Walther and K. W. Rothe (Springer, Berlin, 1979), p. 492.

[38] R. Loudon, *The Quantum Theory of Light* (Clarendon, Oxford, 1973), especially Chap. 9.